MULTI-LAYER DIFFUSION APPROXIMATION FOR PHOTON TRANSPORT IN BIOLOGICAL TISSUE

A Thesis

by

JOSEPH HOLLMANN

Submitted to the Office of Graduate Studies of
Texas A&M University
in partial fulfillment of the requirements for the degree of

MASTER OF SCIENCE

August 2007

Major Subject: Biomedical Engineering

MULTI-LAYER DIFFUSION APPROXIMATION FOR PHOTON TRANSPORT IN BIOLOGICAL TISSUE

A Thesis

by

JOSEPH HOLLMANN

Submitted to the Office of Graduate Studies of
Texas A&M University
in partial fulfillment of the requirements for the degree of

MASTER OF SCIENCE

Approved by:

Chair of Committee, Lihong V. Wang
Committee Members, Alvin T. Yeh
Marvin L. Adams
Head of Department, Gerald Cote

August 2007

Major Subject: Biomedical Engineering

ABSTRACT

Multi-Layer Diffusion Approximation for Photon Transport in Biological Tissue.

(August 2007)

Joseph Hollmann, B.S., Northeastern University

Chair of Advisory Committee: Dr. L. V. Wang

A method for improving the accuracy of the optical diffusion theory for a multi-layer scattering medium is presented. An infinitesimally narrow incident light beam is replaced by multiple isotropic point sources of different strengths that are placed in the scattering medium along the incident beam. The multiple sources are then used to develop a multi-layer diffusion theory. Diffuse reflectance is then computed using the multi-layer diffusion theory and compared with accurate data computed by the Monte Carlo method. This multi-source method is found to be significantly more accurate than the previous single-source method. The appendix to this thesis also shows the derivation of the extrapolated boundary condition. This boundary condition is utilized to solve for the discontinuity that occurs at the tissue-ambient medium interface. The boundary conditions for common index of refraction mismatches are solved for and listed in a table.

.

TABLE OF CONTENTS

Page

ABSTRACT…….. iii

TABLE OF CONTENTS……..…… iv

LIST OF FIGURES…….. v

1. INTRODUCTION: BACKGROUND…….. 1

1.1 Current Knowledge……. 2

2. THEORY…….. 3

2.1 Setup…… 3
2.2 Semi-infinite Medium…….…… 3

3. TWO-LAYER……... 6

3.1 Boundary Conditions…….. 7
3.2 Simulation……... 11

4. EXPERIMENTAL DESIGN…… 13

4.1 Results…… 13

5. OBLIQUE INCIDENCE…….. 17

5.1 Results…… 20

6. CONCLUSIONS……. 22

REFERENCES…… 23

APPENDIX……. 25

VITA……..……. 29

.

LIST OF FIGURES

FIGURE Page

1 Positions of isotropic point sources in a two-layer medium.…….……..…….. 6

2A Comparison of diffuse reflectance calculated with single-source (dotted line), double-source approximations (solid line) and with that calculated with the Monte Carlo method (circles)..……. 14

2B The absolute value of the relative error for the single-source (dotted line) and double-source (solid line) diffusion approximations…… 15

3A Comparison of diffuse reflectance calculated with the double-source approximation (solid line) and with the Monte Carlo method (circles)……. 16

3B The relative error for the double-source diffusion approximation….. 17

4 An infinitesimally narrow beam is incident upon a two-layer turbid medium at an angle θ_i and enters the medium at θ_{t1}……..... 18

5 Comparison of diffuse reflectance calculated with the double-source approximation (solid line) and with Monte Carlo (circles) simulations for a two-layer diffuse medium…… 21

.

INTRODUCTION: BACKGROUND

Characterizing the spectral and spatial properties of biological tissue can yield information about its physiological parameters.[1] These physiological properties, in turn, can be used to monitor tissue metabolic status or diagnose disease such as cancer. Since light interacts with tissue at a sub-cellular level, changes in these interactions can indicate the presence of cancer or other diseases. Dermatologists have acknowledged the importance of optical absorption in analyzing skin lesions by including color ABCD (Asymmetry, Border, Color and Dimension) method for skin cancer diagnosis.[2] This method is used to qualitatively characterize a lesion based on parameters known to be correlated to skin cancer.

However this is a qualitative method of diagnosis and can vary from doctor to doctor. Also, this method is used as a screening technique to identify suspicious lesions. After the initial screening, the gold standard for testing a suspicious lesion is a biopsy. This requires a portion of the lesion to be removed and sent off to a lab to be analyzed; a process that can take weeks. There is also a practical limit to the maximum number of biopsies that can be collected from a patient with multiple suspicious lesions. This can lead to sites identified through the ABCD method as possibly cancerous to go untested. There is also the concern of disfiguring scars associated with the procedure.

However, with the advent of the field of tissue optics, there is an interest in quantifying the spectral and spatial properties of tissue and their correlation to skin cancer. This way the detection of skin cancer can be non-invasively and accurately

---

This thesis follows the style of Applied Optics.

.

accomplished by optically identifying indicators of cancer. However, this endeavor is complicated by the fact photons undergo a large number of scattering events while propagating through tissue. Another confounding factor is tissue can be layered with the tissue of interest buried below another layer.

1.1. Current Knowledge

The radiative transport equation describes the propagation of light through a turbid medium such as tissue assuming its polarization and coherence can be ignored. However, a general solution is difficult to obtain so the diffusion approximation to the radiative transport equation is often employed. The resulting diffusion equation is most commonly used with simple boundary conditions such as a semi-infinite, turbid medium with homogenous optical properties. However, fitting this model to measured diffuse reflectance from tissue with a layered structure can return false optical properties[3] and hence provide a misleading diagnosis of the tissue's health or metabolic activity.

A solution to the diffusion equation for a two-layer medium has been proposed but stipulates a single equivalent point source (to be discussed below) is located within the first layer; which minimizes the influence of a secondary layer on the resulting diffusely reflected signal. This stipulation can restrict the situations in which the current two-layer diffusion equation can be accurately utilized.

.

2. THEORY

2.1 Setup

The problem of interest has an infinitesimally narrow, collimated light beam that is incident perpendicularly upon the surface of the tissue. The coordinate system is set up so the origin is located at the point where the beam enters the medium; its *z*+ axis points down. The incident beam is replaced by an equivalent isotropic point source in each layer of the turbid medium (to be discussed below). The ambient and turbid media are assumed to have matched indices of reflection. The spatially resolved, diffusely reflected signal from the medium is collected.

2.2 Semi-infinite Medium

Light transport through tissue can be described using the scattering (μ_s) and absorption coefficients (μ_a) and the anisotropy factor (g). The coefficients, μ_s and μ_a, describe the probabilities of scattering and absorption per unit infinitesimal length, respectively. The anisotropy factor is the mean cosine of the scattering angle[4]. Most biological tissue is highly forward scattering ($g > .8$). The anisotropic dependent scattering coefficient of the medium can be replaced by an equivalent isotropic transport or reduced scattering coefficient, given as $\mu_s' = \mu_s(1-g)$, in the diffusion regime[5].

In general, tissue has a high reduced scattering coefficient and a low absorption coefficient; which means a photon is likely to undergo many scattering events before being absorbed. After multiple scattering events, photons will travel almost equally in all

.

directions so the diffusion approximation to the radiative transport equation can be utilized.

Another approximation states the reflectance from an infinitesimally narrow, collimated beam, incident on the surface of a turbid medium can be represented by an equivalent isotropic point source buried within the medium. This allows the incident source to be removed from further calculations. The diffusion equation for a semi-infinite homogenous medium is

$$\nabla^2\Phi(x,y,z) - \frac{\mu_a}{D}\Phi(x,y,z) = -\frac{w}{D}\delta(x,y,z-z_0) \qquad (1)$$

where Φ is the fluence, w is the equivalent point source strength and $D = \left(3(\mu_s{}'+\mu_a)\right)^{-1}$ is the diffusion constant. The Dirac delta function, located at z_0, is the position of the equivalent point source within the medium.

The location and strength of the equivalent point source is given by the medium's optical parameters. A photon that enters the medium at a normal angle, traveling in the z+ direction, will have an exponentially decaying probability of progressing to a depth z before being either scattered or absorbed. To remove the incident beam from subsequent calculations, each first scattering site in the equivalent isotropic scattering medium produces a point source. A simplifying assumption sums the point sources into a single source radiating with an intensity equal to the transport scattering albedo, given by $a' = \mu_s'/(\mu_s'+\mu_a)$. The source position is given by the intensity-weighted mean of the first-scattered, isotropic sources' positions within the medium. For a semi-infinite medium the position is given by the mean free path

$$L_t' = \frac{1}{\mu_t'} = \frac{1}{\mu_s' + \mu_a}, \qquad (2)$$

.

where μ_t' is the transport interaction coefficient.

As mentioned above, a two-layer model for light propagation through tissue has been developed previously. This model utilizes a single, equivalent isotropic point source with an intensity and location based on the first layer's optical properties.[6] From the discussion above, we can see this method is not correct because it fails to consider the first scattering sites in the second layer.

.

3. TWO-LAYER

For the purposes of our derivations, the tissue will be approximated as a two-layer turbid medium (Figure 1). As stated above, each layer has independent reduced scattering and absorption coefficients. The depth of the boundary between the first and second tissue layers is given by *L*. The boundary between the tissue and ambient medium is treated utilizing the extrapolated boundary condition.[7] For our calculations, we assume the ambient and turbid medium have matched indices of refraction. We model the fluence in the medium and the diffuse reflectance by placing an equivalent source in each layer. These equivalent sources, rather than the incident collimated beam, are used for further computation.

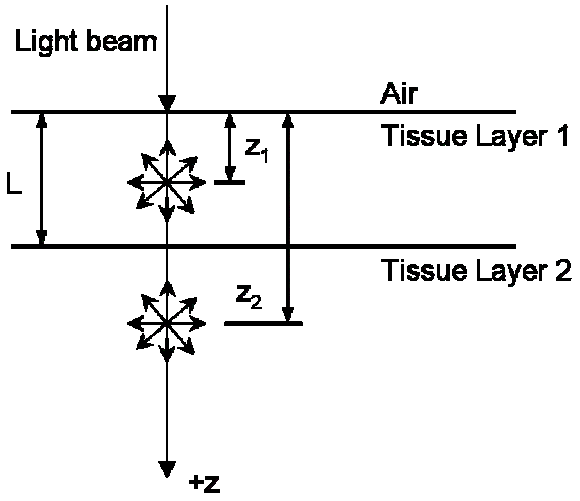

Figure 1 Positions of isotropic point sources in a two-layer medium. The first layer has a thickness of L.

The diffusion equation for a two-layer medium is given as

$$\nabla^2\Phi_i(x,y,z)-\frac{\mu_{ai}}{D_i}\Phi_i(x,y,z)=\frac{-w_i}{D_i}\delta(x,y,z-z_i) \quad i=1,\,2 \quad (3)$$

.

where z_i corresponds to the isotropic point source position in the i^{th} layer.

The equivalent source positions are given by the intensity-weighted mean of the first-scattering locations along the z-axis within each layer:

$$z_1 = \frac{\int_0^L z\exp(-\mu_{t1}' z)dz}{\int_0^L \exp(-\mu_{t1}' z)dz} = \frac{1-(\mu_{t1}' L+1)\exp(-\mu_{t1}' L)}{\mu_{t1}'(1-\exp(-\mu_{t1}' L))}$$
$$z_2 = \frac{\int_L^\infty z\exp(-\mu_{t1}' L-\mu_{t2}'(z-L))dz}{\int_L^\infty \exp(-\mu_{t1}' L-\mu_{t2}'(z-L))dz} = L+\frac{1}{\mu_{t2}'} \quad (4)$$

Each equivalent source is given a radiative intensity or weighting:

$$w_1(z) = \mu_{s1}'\int_0^L \exp(-\mu_{t1}' z)dz = a_1'(1-\exp(-\mu_{t1}' L))$$
$$w_2(z) = \mu_{s2}'\int_L^\infty \exp(-\mu_{t1}' L-\mu_{t2}'(z-L))dz = a_2'\exp(-\mu_{t1}' L) \quad (5)$$

These equations can be compared to the semi-infinite case by setting L equal to zero or infinity.

3.1 Boundary Conditions

The solution to the two-layer diffusion equation requires four boundary conditions to solve for the constants of integration. The extrapolated boundary condition for a matched index of refraction between the turbid and ambient medium is employed. This condition uses the method of images and stipulates a plane of zero fluence located at a distance of z_b above the medium.

.

$$\phi_1(-z_b, s) = 0 \tag{6}$$

Incorporating this into equation 3 yields

$$\phi_1(z = z_b, s) = C_a \exp(\alpha_1 z_b) + C_b \exp(-\alpha_1 z_b) + \frac{w_1}{2\alpha_1 D_1} \exp(-\alpha_1 (z_b + z_1)) = 0 . \tag{7}$$

Another stipulation is the turbid medium extends to infinity along the positive z-axis. Since there is absorption in the medium, the boundary condition can be written as

$$\phi_2(+\infty, s) = 0 . \tag{8}$$

This boundary condition can be solved as follows

$$\lim_{z\to\infty}\left(\phi_2(z,s)\right) = \lim_{z\to\infty}\left(C_c \exp(-\alpha_2 z) + C_d \exp(\alpha_2 z) + \frac{w_2}{2\alpha_2 D_2} \exp(-\alpha_2 (z - z_2)) \right) = 0 , \tag{9}$$

and requires

$$C_d = 0 . \tag{10}$$

We have continuity of the fluence rate at the boundary between the layers assuming a uniform index of refraction in the tissue:

$$\frac{\phi_1(L,s)}{\phi_2(L,s)} = 1 \tag{11}$$

which yields

$$C_a \exp(-\alpha_1 L) + C_b \exp(\alpha_1 L) + \frac{w_1}{2\alpha_1 D_1} \exp(-\alpha_1 (L - z_1)) = C_c \exp(-\alpha_2 L) + \frac{w_2}{2\alpha_2 D_2} \exp(-\alpha_2 (z_2 - L))$$

The flux at the boundary is written as

$$D_1 \left.\frac{\partial \phi_1(z,s)}{\partial z}\right|_{z=L} = D_2 \left.\frac{\partial \phi_2(z,s)}{\partial z}\right|_{z=L} . \tag{12}$$

After computing the derivative, the equation above can be written as

.

$$D_1\left(-\alpha_1 C_a \exp(-\alpha_1 L)+\alpha_1 C_b \exp(\alpha_1 L)-\frac{w_1}{2D_1}\exp(-\alpha_1(L-z_1))\right) = D_2\left(\begin{matrix}-\alpha_2 C_c \exp(-\alpha_2 L)\\ +\frac{w_2}{2D_2}\exp(-\alpha_2(z_2-L))\end{matrix}\right). \tag{13}$$

We see above one constant of integration was already solved for. The rest can be found by solving the following linear system of equations.

$$C = A^{-1}G \tag{14}$$

where the matrix of coefficients, A, is given as

$$A = \begin{vmatrix} \exp(\alpha_1 z_b) & \exp(-\alpha_1 z_b) & 0 \\ \exp(-\alpha_1 L) & \exp(\alpha_1 L) & -\exp(\alpha_2 L) \\ -\alpha_1 D_1 \exp(-\alpha_1 L) & \alpha_1 D_1 \exp(\alpha_1 L) & \alpha_2 D_2 \exp(-\alpha_2 L) \end{vmatrix} \tag{15}$$

the vector of solutions, G, is

$$G = \frac{1}{2}\begin{vmatrix} -\frac{w_1}{\alpha_1 D_1}\exp(-\alpha_1(z_b+z_1)) \\ \frac{w_2}{\alpha_2 D_2}\exp(-\alpha_2(z_2-L))-\frac{w_1}{\alpha_1 D_1}\exp(-\alpha_1(L-z_1)) \\ w_2\exp(-\alpha_2(z_2-L))+w_1\exp(-\alpha_1(L-z_1)) \end{vmatrix} \tag{16}$$

and C contains the constants that will be solved for

$$C = \left|C_a, C_b, C_c\right|^T. \tag{17}$$

Solving for the constants yields the following solution for the first layer

.

$$\phi_1(z,s) = {w_1}\Big/{\alpha_1 D_1}$$

$$\left[\begin{array}{l}
\dfrac{(\alpha_2 D_2 - \alpha_1 D_1)}{(\alpha_2 D_2 + \alpha_1 D_1)\exp(\alpha_1(z+2L+2z_b-z_1)) + (\alpha_1 D_1 - \alpha_2 D_2)\exp(\alpha_1(z-z_1))} + \exp(-\alpha_1|z-z_1|) \\
-\dfrac{(\alpha_1 D_1 + \alpha_2 D_2)}{(\alpha_1 D_1 + \alpha_2 D_2)\exp(\alpha_1(z+z_1+2z_b)) + (\alpha_1 D_1 - \alpha_2 D_2)\exp(\alpha_1(z+z_1-2L))} \\
+\dfrac{(\alpha_1 D_1 - \alpha_2 D_2)}{(\alpha_1 D_1 + \alpha_2 D_2)\exp(\alpha_1(2L-z_1-z)) + (\alpha_1 D_1 - \alpha_2 D_2)\exp(-\alpha_1(z+z_1+2z_b))} \\
+\dfrac{(\alpha_2 D_2 - \alpha_1 D_1)}{(\alpha_1 D_1 + \alpha_2 D_2)\exp(\alpha_1(z_1+2z_b+2L-z)) + (\alpha_1 D_1 - \alpha_2 D_2)\exp(\alpha_1(z_1-z))}
\end{array}\right]$$

$$+\frac{w_2 \exp(-\alpha_2(z_2-L))\sinh(\alpha_1(z_b+z))}{\alpha_2 D_2 \sinh(\alpha_1(z_b+L)) + \alpha_1 D_1 \cosh(\alpha_1(z_b+L))}$$

$$z \le L$$

and the following for the second layer

$$\phi_2(z,s) = \frac{(\alpha_2 D_2 w_1 \exp(-\alpha_1(L-z_1)) - \alpha_1 D_1 w_2 \exp(-\alpha_2(z_2-L)))}{2(\alpha_2 D_2 \tanh(\alpha_1(z_b+L)) + \alpha_1 D_1)} \frac{\exp(-\alpha_2(z-L))}{\alpha_2 D_2}$$

$$+\frac{(w_2 \exp(-\alpha_2(z_2-L)) + w_1 \exp(-\alpha_1(L-z_1)))\sinh(\alpha_1(L+z_b)) - w_1 \exp(-\alpha_1(z_b+z_1))}{2(\alpha_2 D_2 \sinh(\alpha_1(z_b+L)) + \alpha_1 D_1 \cosh(\alpha_1(z_b+L)))} \exp(-\alpha_2(z-L))$$

$$+\frac{w_2 \exp(-\alpha_2|z_2-z|)}{2\alpha_2 D_2}$$

$$z > L \qquad (18)$$

The solution for the fluence in each layer is the 2-dimensional Fourier Transform of equations above,

$$\Phi_i(x,y,z) = \frac{1}{4\pi^2}\int_{-\infty}^{\infty}\int_{-\infty}^{\infty}\phi_i(z,s)\exp(-i(s_1 x + s_2 y))ds_1 ds_2 \,. \qquad (19)$$

To simplify the calculations, the problem is converted into cylindrical coordinates

$$\Phi_i(\rho,z) = \frac{1}{2\pi}\int_0^{\infty} s\phi_i(z,s)J_0(s\rho)ds \qquad (20)$$

.

where J_0 is a Bessel function of the first kind of the zeroth order, and $\rho=x^2+y^2$. This integration is non-trivial and cannot be done in closed form. To solve this problem, Simpson's numerical quadrature is utilized. Simpson's rule for integration is written as

$$\int_a^b \phi_i(z,s) \approx \frac{b-a}{6}\left[\phi_i(z,a) + 4\phi_i\left(z, \frac{b+a}{2}\right) + \phi_i(z,b)\right] \qquad (21)$$

where the distance between the limits of integration (*a* and *b*) is assumed to be small. For the Simpson's quadrature the distance is assumed to be small enough so a polynomial of degree three accurately mimics the function.[8]

The fluence rate is then used to solve for the spatially resolved, diffuse reflectance by combining the fluence and flux as follows:

$$R(\rho) = \frac{1}{4}\Phi_1(\rho, z=0) + \frac{1}{2}D_1 \left.\frac{\partial \Phi_1}{\partial z}\right|_{z=0} (\rho, z=0)\,. \qquad (22)$$

As previously mentioned, the solution assumes matched indices of refraction between the ambient and turbid medium.

3.2 Simulation

The solution to the two-layer diffusion equation using multiple sources was programmed in MatLab for two scenarios. It is important to note tissue optical properties are highly variable. For skin, dermatologists use a 6-tier classification technique based on a patient's response to sunlight in an attempt to develop a reproducible assessment of skin's optical properties.[9] A quick inspection of your own skin will reveal body-location-dependent absorption of different wavelengths of light. This makes finding a consensus among researchers on skin's optical properties difficult, especially since most

.

measurements are taken *ex vivo.*[10] For this reason, we state the purpose of our choice of optical properties is to simply illustrate the utility of our model.

.

4. EXPERIMENTAL DESIGN

To verify our results, we utilize Monte Carlo simulations as a "gold" standard.[11] A Monte Carlo simulation uses random numbers and weightings based on a medium's optical properties to propagate photon packets. Due to the statistical nature of the Monte Carlo method, a large number of photons must be simulated to achieve acceptable confidence intervals for the results. I have chosen to use ten million photons to verify the diffusion approximation for normal incidence and fifty million photons for oblique incidence. It is important to note the Monte Carlo has been extensively tested with experimental results and its accuracy has been well established.[12] By using a Monte Carlo we eliminate the uncertainty and error associated with experiments. It is also quicker and cheaper to implement a Monte Carlo simulation.

The Monte Carlo code was run on my personal laptop, usually overnight. Calculating the reflectance curve for a turbid medium illuminated by normal incidence usually took about one and a half hours while oblique incidence required fifteen hours.

4.1 Results

Both the single-source and double-source approximations are tested in two cases. First, the thickness of the first layer is greater than one transport mean free path ($L > 1/\mu_{t1}'$). In other words, the first layer is optically thick. In this case, we can test the single-source solution against the two-source solution. The parameters used are $\mu_{s1}=90$ cm^{-1}, $\mu_{a1}=0.02$ cm^{-1}, $\mu_{s2}=110$ cm^{-1}, $\mu_{a2}=0.1$, $g=0.9$ and L =0.12 cm. Figure 2A shows the diffuse reflectance, as calculated from these parameters, for distances up to 0.5 cm from

.

the source. Figure 2A shows good agreement between the Monte Carlo results and both diffusion models. However, if we analyze the absolute relative error relative error between the Monte Carlo reflectance and the diffusion models (Figure 2B), we see the two-source model has a smaller relative error than the single-source model. On average, the relative error for the two-source model is half of the single source model.

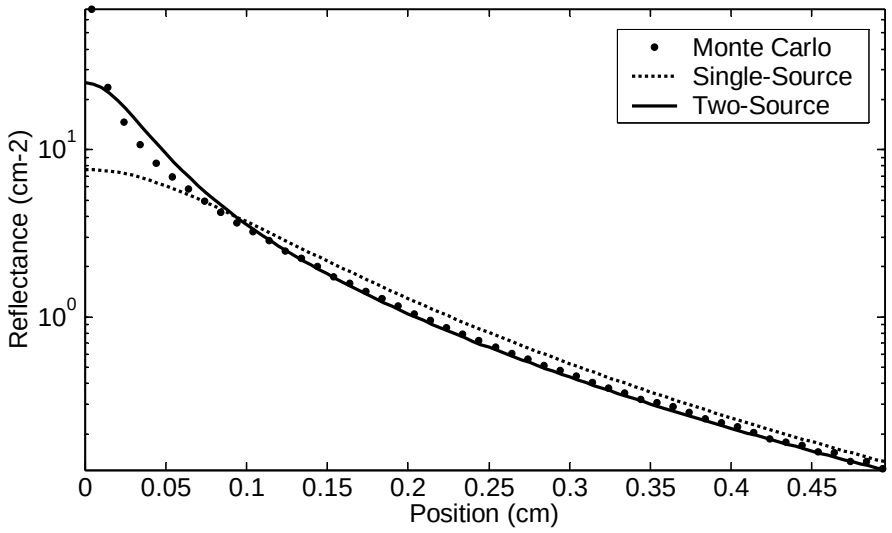

Figure 2A Comparison of diffuse reflectance calculated with single-source (dotted line), double-source approximations (solid line) and with that calculated with the Monte Carlo method (circles). The first layer is optically thick.

.

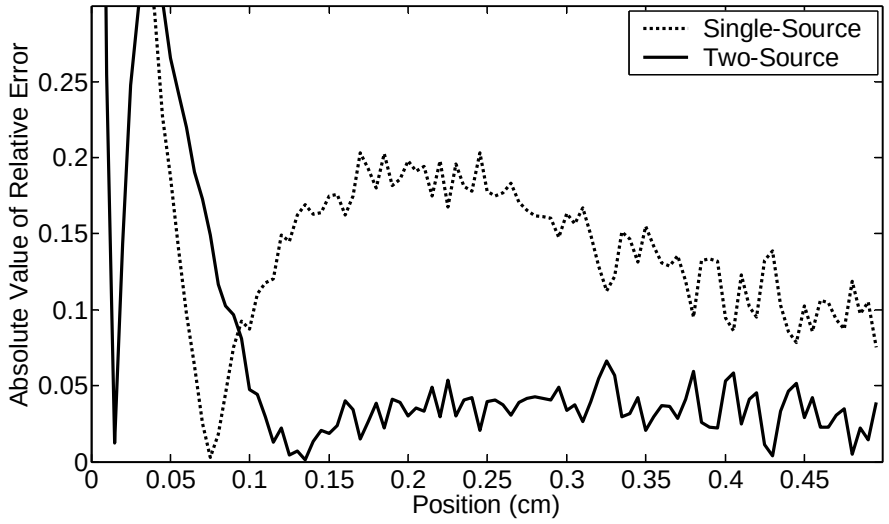

Figure 2B The absolute value of the relative error for the single-source (dotted line) and double-source (solid line) diffusion approximations.

Second, the thickness of the first layer is less than one transport mean free path ($L < 1/\mu_{t1}'$). In other words, the first layer is considered optically thin. In this case, the single-source model is not applicable; but the two-source model still applies since it is not limited by the thickness of the first layer as is the single-source model. The parameters used are $\mu_{s1}=90$ cm^{-1}, $\mu_{a1}=0.02$ cm^{-1}, $\mu_{s2}=110$ cm^{-1}, $\mu_{a2}=0.1$ cm^{-1}, $g=0.9$ and L = 0.06 cm. The results (Figure 3A) show the two-source solution closely follows the Monte Carlo results. A plot of the relative error (Figure 3B) shows the two-source solution has a relative error of less than five percent and has an average error of around 2 percent.

.

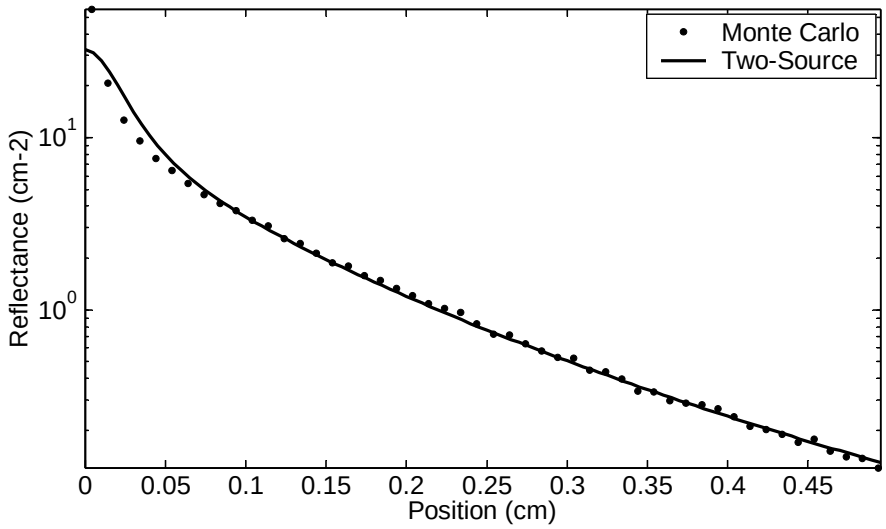

Figure 3A Comparison of diffuse reflectance calculated with the double-source approximation (solid line) and with the Monte Carlo method (circles). The first layer is optically thin.

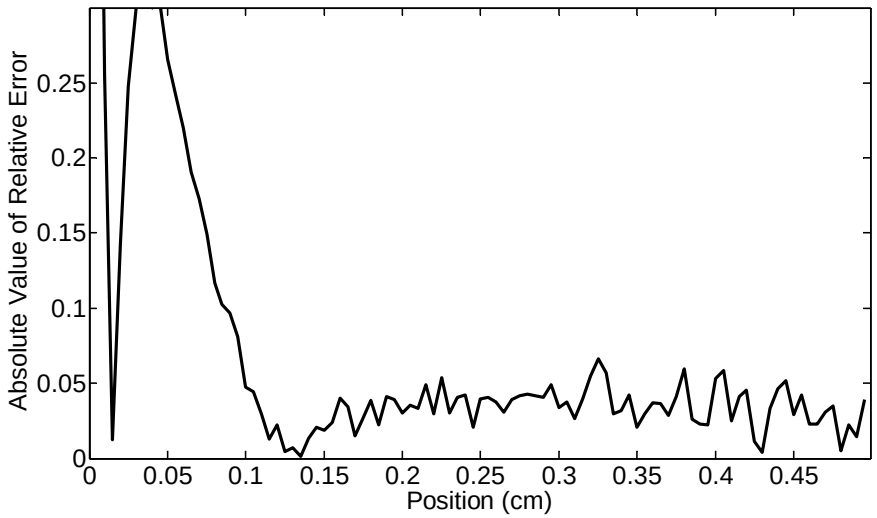

Figure 3B The relative error for the double-source diffusion approximation.

.

5. OBLIQUE INCIDENCE

The method above describes the spatially resolved, diffuse reflectance due to a normally incident pencil beam using the two-layer diffusion approximation to the Radiative Transport Equation. However, Wang et al. [13] showed utilizing an obliquely incident beam offers an improvement over normal incidence. It was shown illuminating a turbid medium with oblique incidence yields the reduced scattering coefficient through measuring the offset of the peak of the diffusion curve from the entry point of the source. Lin et al. [14] showed the absorption coefficient could be recovered as well. This section will lay the ground work for utilizing the two-layer diffusion equation to solve for obliquely incident light.

The problem of interest has a collimated light beam incident upon tissue at an angle, θ_i as shown in Figure 4. The origin of the coordinate system is taken to be the point of incidence, with the z-axis pointing into the tissue. First, we shall approximate tissue as a two-layer turbid medium where the first layer has a thickness, L, and the second layer extends to infinity. For the specific example of skin, these two layers can be considered equivalent to the epidermis and dermis layers.

.

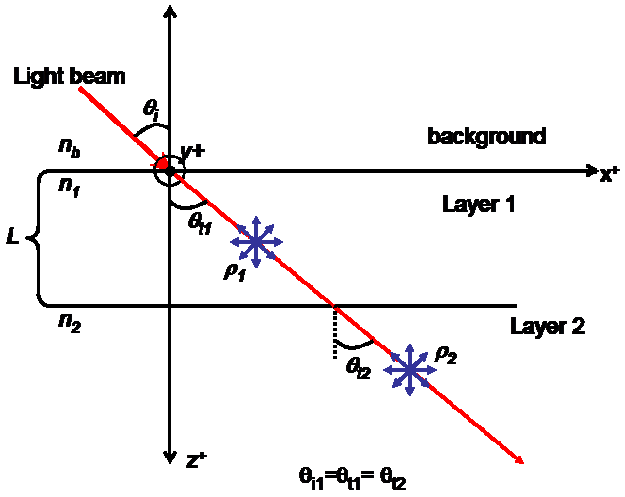

Figure 4 An infinitesimally narrow beam is incident upon a two-layer turbid medium at an angle θ_i and enters the medium at θ_{t1}. The beam is converted into two-equivalent isotropic point sources embedded at locations ρ_1 and ρ_2 along the transmission axis.

The medium is assumed to be index matched with the surrounding medium so the photons' trajectory angle does not change as they are transmitted into the tissue. If this was not the case, we would use Snell's law to describe the transmission angle of light into the turbid medium as follows

$$\theta_t = a\sin\left(n_1 / n_b\right)\sin(\theta_i)) \tag{23}$$

The incident light source is replaced with an equivalent isotropic point source buried within each layer along the transmission axis. These equivalent sources and not the incident beam will be used for further calculations.

The equivalent source positions are given by the intensity weighted mean of the isotropic point sources that approximate the first scattering events along the axis of transmission within each layer,

.

$$\rho_1 = \frac{\int_0^R r\exp(-\mu_{t1}' r)dr}{\int_0^R \exp(-\mu_{t1}' r)dr} = \frac{1-(\mu_{t1}' R+1)\exp(-\mu_{t1}' R)}{\mu_{t1}'(1-\exp(-\mu_{t1}' R))}$$
$$\rho_2 = \frac{\int_R^\infty r\exp(-\mu_{t1}' R-\mu_{t2}'(r-R))dr}{\int_R^\infty \exp(-\mu_{t1}' R-\mu_{t2}'(r-R))dr} = R+\frac{1}{\mu_{t2}'} \quad (24)$$

where ρ_i Euclidian distance from the origin. The corresponding positions along the *x*- and *z-axis* are given by

$$x_i = \rho_i \sin(\theta_{ti})$$
$$z_i = \rho_i \cos(\theta_{ti}) \quad (25)$$

The two-layer diffusion equation for obliquely incident light looks similar to equation **4** except for the source term is now located at $(x_i, 0, z_i)$

$$\nabla^2\Phi_i(x,y,z) - \frac{\mu_{ai}}{D_i}\Phi_i(x,y,z) = \frac{-w_i}{D_i}\delta(x-x_i, y, z-z_i) \quad i=1, 2 \quad (26)$$

The two-dimensional Fourier Transform of this equation yields

$$\frac{\partial^2}{\partial z^2}\phi_i(z,s_a,s_b) - \alpha_i^2\phi_i(z,s_a,s_b) = -\frac{w_i}{D_i}\delta(x-x_i, z-z_i) \quad (27)$$

This problem can be solved for in a similar manner as above. The result, similar to equation 19 is

$$\Phi_i(x,y,z) = \frac{1}{4\pi^2}\int_{-\infty}^{\infty}\int_{-\infty}^{\infty}\phi_i(z,s)\exp(-i(s_1x+s_2y))ds_1ds_2\,. \quad (28)$$

However, the resulting equation for the fluence within the first layer is not radially symmetric. This means equation 20 cannot be directly utilized.

.

However, it should be noted the fluence in both layers is a result of a linear combination of each individual source's contribution or

$$\begin{aligned}\Phi_i(x,y,z) &= \frac{1}{4\pi^2}\int_{-\infty}^{\infty}\int_{-\infty}^{\infty}\big(\mathrm{X}(z,s)+\mathrm{Y}(z,s)\big)\exp(-i(s_1x+s_2y))ds_1ds_2 \\ &= \frac{1}{4\pi^2}\int_{-\infty}^{\infty}\int_{-\infty}^{\infty}\mathrm{X}(z,s)\exp(-i(s_1x+s_2y))ds_1ds_2 \\ &\quad+\frac{1}{4\pi^2}\int_{-\infty}^{\infty}\int_{-\infty}^{\infty}\mathrm{Y}(z,s)\exp(-i(s_1x+s_2y))ds_1ds_2\end{aligned} \quad . \quad (29)$$

where X(z,s) and Y(z,s) are the contributions of the first and second source respectively. We see each individual source can be solved for separately.

5.1 Results

To test the model, the diffusion equation for an infinitesimally narrow beam of light incident upon a two-layer turbid medium at an oblique angle was programmed in MatLab. The geometry of the problem is shown in Figure 4. As in previous work[13,14] the detectors have an offset (Δy) on the y-axis, in a plane parallel to the incident beam. A Monte Carlo simulation of photons propagating through a two-layer turbid medium with set optical properties was also programmed for comparison purposes.

The medium was assumed to have the following optical properties: μ_{a1}=0.05 cm^{-1}, μ_{a2}=0.1 cm^{-1}, μ_{s1}=110 cm^{-1}, μ_{s2}=90 cm^{-1}, L = 0.6 cm and g = 0.9 for both layers. The detectors were assumed to be located at Δy =0.15 cm. It was assumed the light was incident on the medium at a 45 degree angle to the normal. The results of both the oblique incidence diffusion equation and the Monte Carlo simulations are shown in Figure 5. The figure shows the peak of the diffuse

.

reflectance curve is offset from the origin on the *x*-axis. Previously, this offset, Δx, has been used to predict the reduced scattering coefficient of a semi-infinite turbid medium[13].

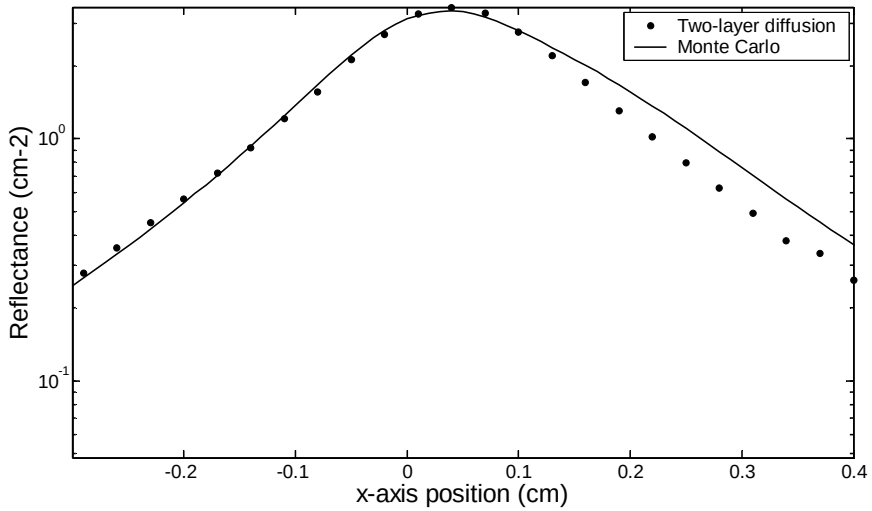

Figure 5 Comparison of diffuse reflectance calculated with the double-source approximation (solid line) and with Monte Carlo (circles) simulations for a two-layer diffuse medium.

.

6. CONCLUSIONS

This thesis has introduced a novel technique for solving for the diffuse reflectance from a multi-layer turbid medium. Our solution stipulates the fluence rate inside a multi-layer medium can best be modeled by multiple, equivalent, isotropic point sources. For illustrative purposes, Appendix A describes the solution to the diffusion equation for two layers.

The method was then validated with Monte Carlo simulations and tested against the single-source, two-layer solution for an optically thick layer. Figures 2A and 2B illustrate the two-source approximation performs better than the single-source solution. We see the two-source model has an average relative error that is less than half of the error for the single source. The results in Figures 3A and 3B show the two-source approximation is also accurate for an optically thin first layer. In contrast, the single-source solution can not be used for this situation. It can be shown from the equations above as the thickness of layer 1 approaches zero, so does the strength of the source embedded within its medium. Therefore, we can see that the two-source solution is valid at any thickness of layer 1. By removing this dependency, we have created a much more robust solution for the diffusion equation for a two-layer turbid medium.

The two-layer diffusion equation was then altered to solve for the diffuse reflectance from a beam incident upon a turbid medium at an oblique angle. The results in Figure 5 show the equation does not match the results from a Monte Carlo simulation. The primary reason is the diffusion equation predicts an asymmetric curve around some position, Δx. The Monte Carlo results clearly show no such asymmetry.

.

REFERENCES

[1.] R. Richards-Kortum, and E. Sevick-Muraca, "Quantitative optical spectroscopy for tissue diagnosis," Annu Rev Phys Chem **11** 555-606 (1996).

[2.] A. Bono, S. Tomatis, C. Bartoli, G. Tragni, G. Radaelli, et al., "The ABCD System of Melanoma Detection: A Spectrophotometric Analysis of the Asymmetry, Border, Color, and Dimension," Cancer **85** (1), 72-77 (1999).

[3.] T. J. Farrell, M. S. Patterson, and M. Essenpreis, "Influence of layered tissue architecture on estimates of tissue optical properties obtained from spatially resolved diffuse reflectometery," Applied Optics **37** (10), 1958-1972 (1998).

[4.] M. J. C. Van Gemert, S. L. Jacques, H. J. C. M. Sterenborg, and W. M. Star, "Skin optics," IEEE Transactions on Biomedical Engineering. **36**, 1146-1154 (1989).

[5.] T. J. Farrell, M. S. Patterson and B. Wilson, "A diffusion theory model of spatially resolved, steady-state diffuse reflectance for the noninvasive determination of tissue optical properties *in vivo*," Med. Phys. **19**, 879-888 (1992).

[6.] A. Kienle, M. S. Patterson, N. Dognitz, R. Bays, G. Wagnieres, and H. Van Den Bergh, "Noninvasive determination of the optical properties of two-layered turbid media," Appl. Opt **37**, 779-791 (1998).

[7.] R. C. Haskell, L. O. Svaasand, T. T. Tsay, T. C. Feng, M. McAdams, and B. J. Tromberg, "Boundary conditions for the diffusion equation in radiative transfer," J. Opt. Soc. Am A, **11**, 2727-2741 (1994).

[8.] D. Kincaid and W. Cheney, "Chapter 7: Numerical differentiation and integration," in *Numerical Analysis: Mathematics of Scientific Computing 3rd edition* (Brooks/Cole, Pacific Grove, CA), 465-519.

[9.] M. A. Pathak, J. Kimbov, G. Szabo, and T. B. Fitzpatrick, “Sunlight and melanin pigmentation,” Photochemical and Photobiological Reviews. **1** 211–239 (1976).

[10.] W. F. Cheong, “Appendix to chapter 8: Summary of optical properties,” in *Optical-Thermo Response of Laser-irradiated Tissue*, A. J. Welch and M. J. Van Gemert, eds. (Plenum Press, NY, 1995), 275-303.

[11.] L.-H. Wang, S. L. Jacques, and L.-Q. Zheng, “MCML - Monte Carlo modeling of photon transport in multi-layered tissues,” Computer Methods and Programs in Biomedicine **47**, 131-146 (1995).

[12.] S. T. Flock, B. C. Wilson, and M. S. Patterson, “Monte Carlo modeling of light propagation in highly scattering tissues — II: comparison with measurements in phantoms,” IEEE Trans. Biomed. Eng. **36** 1169–1173 (1989).

[13.] L.-H. Wang and S. L. Jacques, “Use of a laser beam with an oblique angle of incidence to measure the reduced scattering coefficient of a turbid medium,” Applied Optics **34**, 2362-2366 (1995).

[14.] S.-P. Lin, L.-H. Wang, S. L. Jacques, and F. K. Tittel, “Measurement of tissue optical properties using oblique incidence optical fiber reflectometry,” Applied Optics **36**, 136-143 (1997).

APPENDIX

The purpose of this thesis has been to introduce a new and more accurate model to solve for diffuse light traveling through a turbid medium. The extrapolated boundary condition was utilized without discussion to solve for the fluence in and the reflectance from the turbid medium. For the sake of simplicity, the discussion above was constrained to a situation where the ambient and turbid media have matched indices of refraction. However, this is not realistic for tissue-air interfaces likely to be encountered when modeling the fluence of light through skin.

The extrapolated boundary condition is most commonly used to compensate for the ambient-turbid media boundary. However, it has been pointed out many researchers have incorrectly used a mixture of boundary conditions or incorrectly employed this boundary condition when solving the diffusion equation. A detailed approach deriving and explaining how to correctly utilize the extrapolated boundary condition can be found elsewhere[7]. This appendix seeks to simplify their work and create a reference table that can be referenced when solving the diffusion equation for a semi-infinite medium. To this end, we will briefly discuss the derivation of the boundary condition and present some results for common index mismatches.

The extrapolated boundary condition uses the method of images to solve for the tissue-ambient media interface. The condition assumes there is a plane where the fluence is equal to zero at a given distance from the boundary within the ambient medium. A detailed discussion and derivation of this boundary condition can be found in more detail elsewhere[7]. The purpose of this appendix is to illustrate how to calculate the necessary parameters to utilize the boundary conditions.

As mentioned above, the diffusion equation assumes unpolarized light is traveling through the medium. The Fresnel coefficient for unpolarized light solves for the probability of light propagating over a boundary for a given incident angle.

$$R_{fres}(\theta_m) = \begin{cases} \frac{1}{2}\left(\frac{n_m \cos(\theta_t) - n_a \cos(\theta_i)}{n_m \cos(\theta_t) + n_a \cos(\theta_i)}\right)^2 + \frac{1}{2}\left(\frac{n_m \cos(\theta_i) - n_a \cos(\theta_t)}{n_m \cos(\theta_i) + n_a \cos(\theta_t)}\right)^2 & 0 \le \theta \le \theta_c \\ 1 & \theta_c \le \theta \le \pi/2 \end{cases} \quad \text{(A1)}$$

where the indicies of refraction for the ambient and turbid media are n_a and n_m respectively. The incident angle (θ_i) refers to the angle the photon hits the boundary at. The transmitted angle (θ_t) is found with Snell's law

$$n_a \sin(\theta_t) = n_m \sin(\theta_i) \quad \text{(A2)}$$

Photons incident upon the medium at an angle greater than the critical angle, given by

$$\theta_c = a\sin\left(\frac{n_a}{n_m}\right), \quad \text{(A3)}$$

are assumed to be internally reflected.

The radiance or intensity of light is written as

$$L(\vec{r}, \hat{s}) = \frac{1}{4\pi}\Phi(\vec{r}) + \frac{3}{4\pi} j(\vec{r}) \bullet \hat{s} \quad \text{(A4)}$$

where $\Phi(\vec{r})$ is the fluence and $j(\vec{r}) = -D\nabla\Phi(\vec{r})$ is the flux and $\hat{s} = (\sin\theta\cos\phi, \sin\theta\sin\phi, \cos\theta)$ is an unit directional vector and points into the turbid medium.

The irradiance at the tissue-ambient media boundary is set equal to the sum of the reflected radiance

$$E_{irrad} = \iint_{\hat{s}\bullet\hat{n}>0} L(\hat{s})\hat{s} \bullet R_{fres}(\hat{n}) d\Omega \quad \text{(A5)}$$

where $\hat{n} = -\hat{z}$ points out of the turbid medium.

The left hand side of the equation above or irradiance at the boundary is written as

$$E_{irrad} = \iint_{\hat{s}\bullet\hat{n}<0} L(\hat{s})\hat{s}\bullet(-\hat{n})d\Omega = \frac{\Phi}{4} + \frac{j_z}{2} \tag{A6}$$

Equation (A5 can be used to write the reflected radiance from the medium as

$$\iint_{\hat{s}\bullet\hat{n}>0} R_{fres}(\hat{s})L(\hat{s})\hat{s}\bullet(-\hat{n})d\Omega = R_\Phi \frac{\Phi}{4} - R_j \frac{j_z}{2} \tag{A7}$$

where

$$\begin{aligned} R_\Phi &= 2\int_0^{\pi/2} R_{fres}(\theta)\sin(\theta)\cos(\theta)d\theta \\ R_j &= 3\int_0^{\pi/2} R_{fres}(\theta)\sin(\theta)\cos^2(\theta)d\theta \end{aligned} \quad . \tag{A8}$$

The effective reflection coefficient can be written as follows

$$R_{eff} = \frac{R_\Phi + R_j}{2 - R_\Phi + R_j} \tag{A9}$$

The effective reflection coefficient can be used to find the *z*-axis position of the zero-fluence plane as follows

$$A = \frac{1 + R_{eff}}{1 - R_{eff}} \tag{A10}$$

$$z_b = 2AD\,. \tag{A11}$$

The effective reflection coefficient represents the percentage of the emittance that is reflected and becomes the irradiance.

The spatially resolved reflectance can be written as follows

$$R(\rho) = \frac{1}{4\pi}\int_{2\pi}\left(1 - R_{fres}(\theta)\right)\times\left(\Phi(\rho, z=0) + 3D\frac{\partial\Phi(\rho, z=0)}{\partial z}\cos(\theta)\right)\times\cos(\theta)d\Omega \tag{A12}$$

or if we change the coordinate system and let $T(\theta) = \left(1 - R_{fres}(\theta)\right)$ we get

$$R(\rho) = \frac{\Phi(\rho, z=0)}{4\pi}\int_{\pi} T(\theta)\cos(\theta)\sin(\theta)d\theta\int_{2\pi} d\varphi + \frac{3D}{4\pi}\frac{\partial\Phi(\rho, z=0)}{\partial z}\int_{\pi} T(\theta)\cos(\theta)\cos(\theta)\sin(\theta)d\theta\int_{2\pi} d\varphi$$

$$= \frac{\Phi(\rho, z=0)}{2}\int_{\pi} T(\theta)\cos(\theta)\sin(\theta)d\theta + \frac{3D}{2}\frac{\partial\Phi(\rho, z=0)}{\partial z}\int_{2\pi} T(\theta)\cos^2(\theta)\sin(\theta)d\theta \quad \text{(A13)}$$

This can be solved easily using Simpson's numerical integration. A list of values for varying indices of refraction mismatches at the ambient-turbid media interface are found in Table 1.

Table 1 List of extrapolated boundary condition parameters for common index of refraction mismatches

	Relative index of reflection							
	1	1.33	1.37	1.4	1.48	1.5	1.54	1.6
r_{Φ}	0	0.4719	0.5055	0.5289	0.5839	0.5962	0.6196	0.6509
r_j	0	0.3282	0.3634	0.3887	0.4501	0.4642	0.4915	0.5288
r_{eff}	0	0.4311	0.4677	0.4934	0.5541	0.5676	0.5936	0.6282
t_{Φ}	0.2500	0.1319	0.1236	0.1178	0.1040	0.1009	0.0950	0.0872
t_j	0.5000	0.3357	0.3182	0.3057	0.2749	0.2678	0.2541	0.2354

VITA

Name: Joseph Hollmann

Address: 4784 Oak St. Apt 344
Kansas City, MO 64112

E-mail Address: Joseph_Hollmann@neo.tamu.edu

Education: B.S., Electrical Engineering, Northeastern University, 2003

M.S., Biomedical Engineering, Texas A&M University, 2007